

## Experimental Assessment of Human Blockage at sub-THz and mmWave Frequency Bands

Juan E. Galeote-Cazorla, Alejandro Ramírez-Arroyo, José-María Molina-García-Pardo, María-Teresa Martínez-Inglés, and Juan F. Valenzuela-Valdés

**Abstract**—The fifth generation (5G) of mobile communications relies on extremely high data transmissions using a large variety of frequency bands, such as FR1 (sub-6 GHz) and FR2 (mmWave). Future mobile communications envisage using electromagnetic spectrum beyond FR2, i.e. above 100 GHz, known as sub-THz band. These new frequencies open up challenging scenarios where communications shall rely on a major contribution such as the line-of-sight (LoS) component. To the best of the authors' knowledge, for the first time in literature this work studies the human blockage effects over an extremely wide frequency band from 75 GHz to 215 GHz given: (i) the distance between the blocker and the antennas and (ii) the body orientation. Furthermore, the obtained results are modeled with the classical path loss models and compared to 3GPP alternatives. The average losses increase from 42 dB to 56 dB when frequency rises from 75 GHz to 215 GHz. In terms of distance, a 18 dB increment in the received power is found when the Tx–Rx separation is increased from 1 m to 2.5 m. Finally, the blocker orientation induces variations of up to 4.6 dB.

**Index Terms**—sub-THz, mmWave, human blockage, channel modeling, diffraction, blockage gain, propagation

### I. INTRODUCTION

The evolution of wireless communication systems is toward higher data rates, system capacities, carrier frequencies, and bandwidths [1], [2]. The current fifth-generation (5G) and the future sixth-generation (6G) of wireless systems consider not only millimeter-waves (mmWave) frequencies but also sub-THz (100 GHz – 300 GHz) and THz (0.1 THz – 10 THz) bands as one of the keys to meet their strict specifications [3].

Systems operating at low frequencies (sub-6 GHz) can rely on the main propagation mechanisms, such as reflection, diffraction, and scattering [4]. In contrast, this is not the case for sub-THz and THz bands. At these frequencies, the electrical dimensions of the objects increase considerably producing a detriment of diffraction effects. Moreover, diffuse scattering becomes more relevant due to the surface roughness. Together, all these particularities result in weaker specular components compared to lower frequencies [5], [6]. These behaviors, in addition to the reduced aperture size of antennas in the THz region, involve that communications must rely on the line-of-sight (LoS) component [7]. In mobile communication scenarios, this contribution can be shadowed occasionally. Since the radius of the first Fresnel zone is proportional to the wavelength, the human body can easily block the LoS.

As consequence of the aforementioned reasons, a growing interest has been raised in assessing the impact of human blockage on the performance of communication systems. Thus, accurate deterministic human body shadowing channel models are needed. Some examples of these models have been proposed at mmWave and THz bands in the state-of-the-art.

For instance, in [8] the received signal power variations are statistically characterized in the time domain caused by human activity affecting 60 GHz indoor short-range wireless links. In [9], the authors provide a simple approach to characterize the effects of scattering by human bodies in the vicinity of a short-range indoor link at 28 GHz, while the link is fully blocked by another body. In [10], human blockage measurements in an anechoic chamber at 15 GHz, 28 GHz, and 60 GHz frequencies employing 15 human subjects of different sizes and weights are presented and an effective 3-D human blockage model as a double-truncated multiple knife-edge (DTMKE) scheme is also proposed.

Indeed, diffraction has been used in many studies to model human shadowing. Knife-edge diffraction (KED) [11], [12] models are commonly used in literature. However, it has the drawback that the 3D models are limited to a geometry based on metallic planes. Furthermore, the scattering path from the human body cannot be separated from the LoS path. The uniform theory of diffraction (UTD) [13] features moderate computational cost and a flexible choice of 3D models including screens, hexagon cylinders, and circular cylinders. Physical optics (PO) approximation features a good accuracy for considering the most detailed circumference of the cross-section (CCS) as a human phantom, but the computational cost is unacceptable for dynamic scenarios. Most of the studies focus on mmWave, and some others are increasing the frequency to sub-THz bands. For example, in [14] authors present the results of the evaluation of reflection and blockage losses due to the human body in the 300 GHz band.

In this work, a study on human blockage of the LoS is performed in a large bandwidth from 75 GHz to 215 GHz including both mmWave and sub-THz frequencies. After a thorough analysis in terms of frequency, distance between the antennas, blocker orientation and human subject; the blockage gain parameter is proposed to evaluate the impact on the LoS signal. Then, it is modeled applying a modified version of classical path loss models as function of frequency and distance alternatively to the geometrical based models. Accurate results are obtained, with reduced standard deviation and high channel predictability. Finally, our proposal is compared with the geometrical models from the 3rd Generation Partnership Project (3GPP) known as 3GPP-A and 3GPP-B [15], implying higher complexity and less accurate results. Quantify the blockage effects in the sub-THz and THz bands is fundamental on the development of personal area network (PAN) and body area network (BAN) systems in future cellular generations.

The rest of the article is organized as follows. Section II presents the measurements acquisition process and their post-processing. Section III analyzes the influence of the frequency, distance between the antennas, blocker orientation and human subject. Then, it presents the applied models and their fit with the experimental results. A comparison with other models from the literature is carried out. Finally, Section IV exposes the conclusions of this work.

### II. MEASUREMENTS ACQUISITION AND PROCESSING

Measurements have been carried out in a laboratory located at the facilities of Universidad Politécnica de Carta-

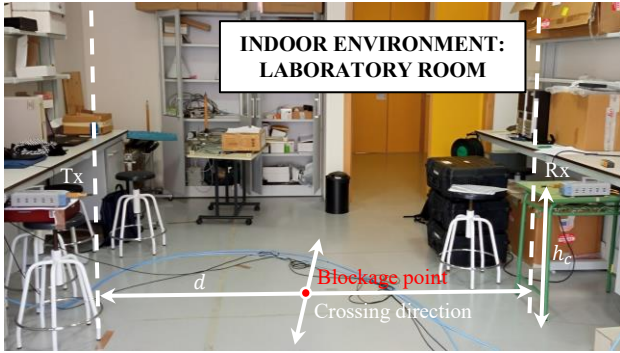


Fig. 1. Panoramic of the measurement setup at UPCT facilities.

gena (UPCT), with a volume of  $8 \times 4.8 \times 3.5 \text{ m}^3$ . The scenario is furnished with desks, chairs, shelves and closets; and it is equipped with several electronic devices such as computers and measurement instruments (see Fig. 1). Transmitter (Tx) and receiver (Rx) are aligned facing each other at a distance  $d \in \{1, 1.75, 2.5\}$  m and at a height above the ground  $h_c = 1$  m. This setup resembles a device-to-device (D2D) communication scenario within an indoor environment, where fading due to human transit is common.

The channel sounder consists of (i) a vector network analyzer (R&S<sup>®</sup> ZVA67) and (ii) several frequency converters (R&S<sup>®</sup> ZVA-Z110E, ZC170 and ZC220) enabling the acquisition in the range from 75 GHz to 220 GHz. The Tx and Rx antennas are standard gain horns (SGHs) of 20 dB gain and a half-power beam width (HPBW) of  $18^\circ$  in H and E planes at mid-band (Flann SGH Series 240 #27240 and #29240). The VNA is configured in continuous wave (CW) mode, with a sampling frequency of 100 Hz (time step of 10 ms). The number of points is set to 2 048, which provides a maximum excess time of 20.47 s. Nine different frequencies are evaluated in the range from 75 GHz to 215 GHz equispaced 17.5 GHz. The most restrictive dynamic range is above 80 dB, and it is observed for the highest frequency, i.e. 215 GHz.

Attending to Fig. 1, the followed methodology consists on a human subject crossing along the perpendicular direction to the Tx–Rx link at its middle point. Two subjects participated in the measurements, performing two blockages crossing head-on and another two in sideways per frequency and distance. Therefore, the total number of captured blockages is 216. At each one, the crossing speed was constant and took a value of 45 cm/s, i.e. 1.62 km/h. It was lower than the typical values for pedestrian speed<sup>1</sup> to emphasize the blockage effects.

One blockage event trace is presented in Fig. 2, captured for a frequency  $f = 75$  GHz, a distance  $d = 1$  m and crossing sideways. The magnitude is normalized to the power of the LoS component (including the antennas gain), which can be seen as a continuous value at the beginning and end of the blockage event. At the central part, the LoS component is completely blocked, which implies a degradation of the received power and an increase in fast fading effects. Additionally, several effects such as arm movements (resulting in partial signal recovery) and diffraction plus reflection interferences

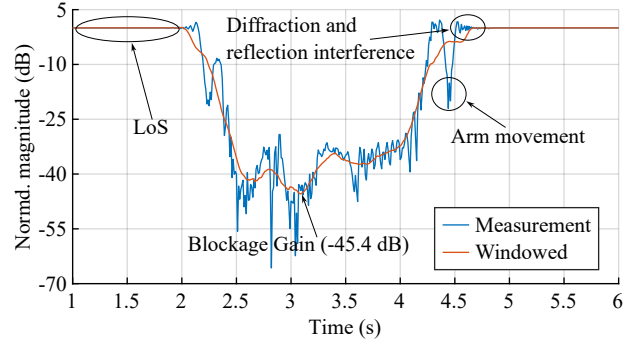


Fig. 2. Example of blockage event measured for  $f = 75$  GHz and  $d = 1$  m (normalized with respect to the LoS component). The red line results from removing the fast fading effects of the measurement.

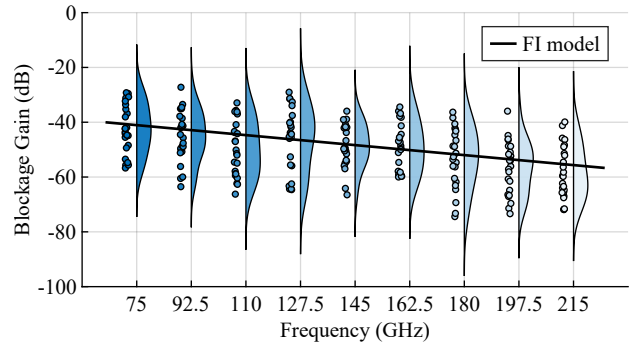


Fig. 3. Blockage gain distribution per studied frequency (violin diagrams). The fit with the modified floating-intercept model is included as a black line.

are observed. In order to characterize the blockage, fast fading effects have to be removed. This can be done applying an averaging over the local mean power with a window size of 36 samples<sup>2</sup> [17]. Then, the concept of blockage gain (BG) naturally arises. We define it as the minimum gain provided by the human along the blockage after removing the fast fading effects. In Fig. 2, blockage gain takes a value of  $-45.5$  dB.

### III. ANALYSIS AND MODELING OF BLOCKAGE GAIN

Applying the aforementioned definition, we have computed the BG parameter for each captured blockage event. Then, it has been analyzed in terms of the factors taken into account in our experiment. As Fig. 3 reveals, the BG follows a clear decreasing trend with frequency. In particular, median values of  $-43.0$  dB and  $-59.7$  dB are obtained for the lowest and highest frequencies respectively (75 GHz and 215 GHz). While the signal attenuation in this frequency range for free space propagation is 9.1 dB, losses of up to 16.7 dB are observed with during the blockage event. This is due to the growth of the blocker electrical dimensions, which intrinsically increases the attenuation with frequency scaling.

An analogous analysis can be performed for the remaining factors. In contrast with the frequency trend, the blockage gain increases as the distance between the antennas is larger. At each configuration (1 m, 1.75 m, and 2.5 m), the median

<sup>2</sup>Given a crossing speed of 45 cm/s, at the lowest studied frequency the window size is equivalent to  $39\lambda$ . This value is within the range from  $20\lambda$  to  $40\lambda$ , which retains the trace slow-fading information [17].

<sup>1</sup>The typical pedestrian speed varies between 4 km/h and 6 km/h [16].

values of BG are  $-59.5$  dB,  $-49.4$  dB, and  $-41.2$  dB respectively; i.e., a 18.3 dB increment from  $d=1$  m to  $d=2.5$  m. In this case, the antennas aperture plays a fundamental role. As distance increases, the blocker relative dimensions are reduced. This favors the diffraction effects around the human body edges.

On the other hand, in terms of the human subject, the discrepancy between the median values is 7.2 dB, which suggests clear differences in their constitutions. Finally, for the body orientation, median values of  $-51.5$  dB and  $-46.9$  dB are obtained in head-on and sideways crossings respectively; i.e. a difference of 4.6 dB. This is a clear consequence of the body extension along the LoS direction, which is higher in the head-on case than in the sideways case.

#### A. Blockage Gain models

In the state-of-the-art, there is a large number of proposals for modeling path loss as a simple function of frequency and distance. However, that is not the case for the blockage losses, which are usually described by the application of diffraction-based models as the DTMKE [10]. They imply a high dependency on the geometrical description of the particular analyzed scenario, which translates into higher complexity.

As mentioned in previous paragraphs, blockage gain has a clear dependence on frequency and distance. These are numerical factors that may derive in regression models, allowing us to describe the blockage gain along the wide spectrum of studied frequencies on the mmWave and sub-THz bands. Seeking a simple description of the blockages behavior, we propose to model the BG with a modified version of the classical path loss models [18]:

- *Floating-intercept (FI)*. Blockage gain is logarithmically frequency-dependent in the form

$$\text{BG}(f) = A + 10n \log_{10} \left( \frac{f}{1 \text{ GHz}} \right) + \chi_{\sigma}, \quad (1)$$

where  $A$  is the intercept, and  $n$  is the loss exponent.

- *Close-in (CI)*. Logarithmic and linear dependencies with frequency and distance, respectively, are assumed. Then,

$$\text{BG}(d, f) = \phi d + 10m \log_{10} \left( \frac{f}{1 \text{ GHz}} \right) + \chi_{\sigma}, \quad (2)$$

where  $\phi$  models the distance-dependent term, and  $m$  represents the frequency loss exponent.

- *Alpha-beta-gamma (ABG)*. It is analogous to the CI model but introduces the intercept parameter  $\beta$ . That is,

$$\text{BG}(d, f) = \alpha d + \beta + 10\gamma \log_{10} \left( \frac{f}{1 \text{ GHz}} \right) + \chi_{\sigma}, \quad (3)$$

where  $\alpha$  is the distance gain factor, and  $\gamma$  is the frequency loss exponent.

- *CI with a frequency-dependent term (CIF)*. This model introduces a cross frequency-distance dependence. Then,

$$\text{BG}(d, f) = a \left( 1 + b \frac{f - f_0}{f_0} \right) d + 10c \log_{10} \left( \frac{f}{1 \text{ GHz}} \right) + \chi_{\sigma}, \quad (4)$$

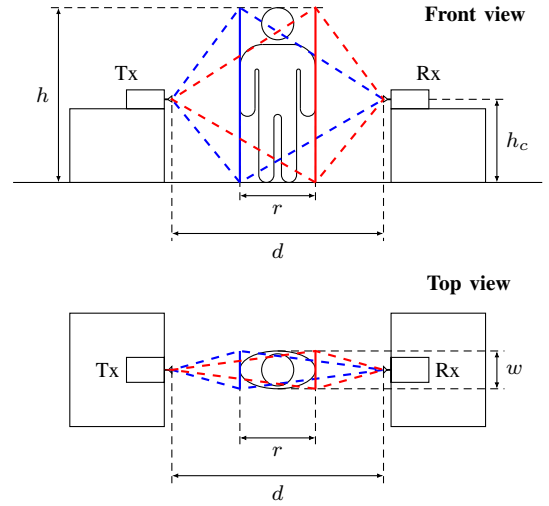


Fig. 4. Geometrical description of the carried out measurements applied to estimate the blockage gain with the 3GPP models. The metallic planes and diffraction paths are represented by solid and dashed lines respectively.

where  $a$  models the distance-dependent term,  $b$  is the cross frequency-distance dependence factor, and  $c$  is the frequency loss exponent. Additionally,  $f_0 = 145$  GHz corresponds to the central frequency of the modeled band.

All the models include a stochastic term  $\chi_{\sigma}$  to capture the factors not taken into account explicitly, i.e. the blocker orientation, the human subject, and other masked influences. It is a zero-mean Gaussian distributed random variable (RV) with variance  $\sigma^2$ .

In order to perform a comparison with geometry-based alternatives, we can also apply the 3GPP blockage models 3GPP-A and 3GPP-B [15]. These are defined for frequencies up to 100 GHz, but can be analytically extended to the upper bound of our range, i.e. up to 215 GHz. The blockage gain estimation is based on modeling diffraction around metallic planes placed in a 3D space. On the one hand, the 3GPP-A model adopts a stochastic approach and only needs to know the angles formed by the Rx and the edges of the planes. On the other hand, the 3GPP-B model adopts a deterministic approach and all the distances between the edges of the metallic planes and both Tx and Rx are needed.

For our particular case, we propose to represent the human blocker as two metallic planes whose height and width are adjusted to the dimensions of the body. Then, the blockage gain can be computed as the sum of their individual contributions. Assuming a standard human, the dimensions of the body are a height  $h = 1.7$  m, a width  $r = 0.4$  m and a depth  $w = 0.3$  m. As can be seen in Fig. 4, we place the blocker completely centered on the Tx–Rx line, where the attenuation is maximum. The metallic planes (red and blue solid lines) are placed at both sides of the body, and their dimensions are of  $w \times h$ . The distance between the antennas is fixed to the corresponding value of  $d$ , and they are on a height  $h_c = 1$  m above the ground. The geometry needed to estimate the blockage gain is completely defined by the diffraction paths represented as red and blue dashed lines. For the 3GPP-A model, we only need to compute the angles between the two paths at the receiver

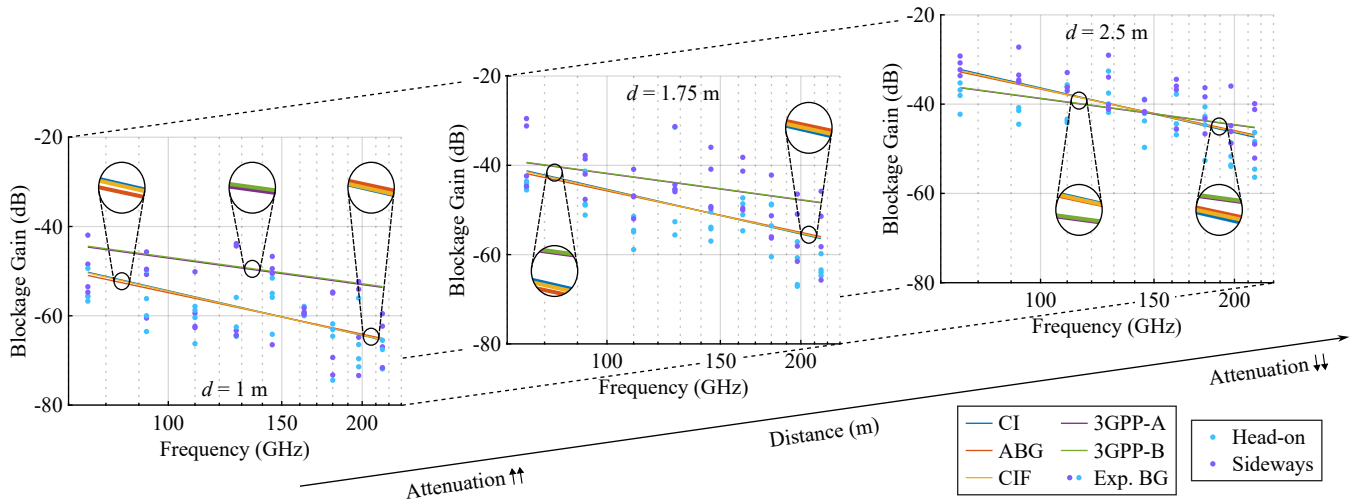


Fig. 5. Comparison between the CI, ABG, and CIF models with the 3GPP-A and 3GPP-B estimations for the three studied distances between the antennas.

side. However, for the 3GPP-B model, the full lengths of all the diffraction paths are required.

### B. Modeling discussion

A fit between the models presented in eqs. (1)–(4) and the BG measurements was carried out applying the least squares method. Thus, the optimal parameters are those which minimize the variance  $\sigma^2$  of the stochastic term  $\chi\sigma$ .

The FI model is the simplest since it only takes into account the operation frequency. However, despite the high dispersion, it is able to properly capture the trend as Fig. 3 shows. An intercept  $A = 16.0$  dB and a loss exponent  $n = -3.09$  are obtained. These results imply that a decade increment in frequency produces a detriment of 30 dB approximately on the received signal. This fact enhances the relevance of human blockage effects at the sub-THz band. At these frequencies, the electrical dimensions of the obstacles increases significantly in comparison with sub-6 GHz and mmWave bands. Therefore, higher penetration losses and impairment of diffraction mechanisms are expected. The minimum standard deviation  $\sigma$  obtained for the model is  $\sigma_{FI} = 9.7$  dB, which is in line with the aforementioned dispersion seen in Fig. 3.

The remaining models introduce the distance between the antennas as an additional variable to the operation frequency. In the case of the CI model, as in the FI one, only two parameters are involved. After perform the fit, the obtained values are  $\phi = 12.0$  dB/m for the distance gain factor and  $m = -3.32$  for the frequency loss exponent. This last parameter is consistent with that obtained for the FI model but slightly higher due to the absence of an intercept parameter. When it is introduced, the ABG model naturally emerges as a generalization of the CI one. For this model, the obtained parameters are a distance gain factor  $\alpha = 12.1$  dB/m, an intercept  $\beta = -5.2$  dB, and a frequency loss exponent  $\gamma = -3.09$ . It now matches that obtained for the FI model, becoming the ABG approach a generalization of both the FI and CI models. Finally, the CIF model modifies the CI one introducing a cross dependence with frequency and distance. The obtained

parameters are a distance gain factor  $a = 12.1$  dB/m, a cross frequency-distance factor  $b = 0.0196$ , and a frequency loss exponent  $c = -3.32$ . Since there is no intercept parameter, the value of  $c$  is equal to that obtained for the CI model. Regarding the parameter  $b$ , it takes a reduced value which suggests that distance and frequency are uncorrelated. This fact explains the similitude between the parameters of the models. In consequence, the obtained  $\sigma$  for each fit are practically the same:  $\sigma_{CI} = 6.18$  dB,  $\sigma_{ABG} = 6.17$  dB, and  $\sigma_{CIF} = 6.17$  dB. The regression curves are presented in Fig. 5, where it can be seen these models practically overlapping with each other. Slight differences are observed in their slopes because of their mathematical expressions and the small changes in the parameters. Nevertheless, the three models properly capture the decreasing trend with frequency and the increasing trend with distance. Another observation is the matching between the distance gain factors  $\phi$ ,  $\alpha$ , and  $a$  from the models CI, ABG and CIF respectively. They take a value near to 12 dB/m, which is explained by the reduced wavelength at the sub-THz bands and the antennas' HPBW. An increase of one meter in distance involves moving the antennas away over several hundred wavelengths. This significantly reduces the relative electrical dimensions of the blocker, which favors the diffraction mechanisms around its edges.

Alternatively to the aforementioned FI, CI, ABG and CIF models, we have also estimated the blockage gain applying the 3GPP-A and 3GPP-B for the geometry presented in Fig. 4. The obtained mean squared errors (MSEs) with respect to the measurements are  $MSE_A = 8.9$  dB and  $MSE_B = 9.0$  dB respectively. Both models results in similar BG values as can be seen in Fig. 5. For a distance  $d = 1$  m, the 3GPP models underestimate the blockage gain by about 10 dB. The difference becomes smaller as distance increases. In the case of  $d = 2.5$  m, these models reasonably approximate the measurements. Therefore, the increase of BG with distance is more restrained for the 3GPP models than the captured by the distance gain factor of the CI, ABG, and CIF models. This behavior is explained attending to the Tx and Rx antennas,



TABLE I  
NUMERICAL VALUES OBTAINED  
AFTER FITTING MEASUREMENTS AND MODELS

FI	CI	ABG	CIF
$A = 16.0$ dB $n = -3.09$	$\phi = 12.0$ dB/m $m = -3.32$	$\alpha = 12.1$ dB/m $\beta = -5.2$ dB $\gamma = -3.09$	$a = 12.1$ dB/m $b = 0.0196$ $c = -3.32$
$\sigma = 9.65$ dB	$\sigma = 6.18$ dB	$\sigma = 6.17$ dB	$\sigma = 6.17$ dB
<b>3GPP-A and 3GPP-B MSEs</b>			
MSE <sub>A</sub> = 8.89 dB		MSE <sub>B</sub> = 8.97 dB	

which are assumed isotropic by the 3GPP models. Under this condition, diffraction effects are favored in short-range compared to the high-directive antennas case. Note that real systems operating at sub-THz bands are expected to introduce highly directive antennas in link-to-link communications to overcome the deep attenuation of these frequencies. Concerning to the frequency dependence, the 3GPP models also underestimate its impact. The loss exponent is clearly lower (in absolute terms) than for the fitted models, which suggests that the effects of blockages are more severe in the sub-THz frequencies than in the mmWave bands.

Finally, all the results obtained from fitting and estimating the blockage gain are summarized in Table I. For our site-specific conditions, the frequency loss exponent is above a value of 30 dB/decade whereas the distance gain factor is about 12 dB/m. A different measurement setup might include the presence of additional contributions to the LoS which could modify these values. For example, a reflection which is not blocked joint with the LoS component would produce a decrease on the frequency loss exponent because it would not be affected by diffraction losses. Additionally, directive antennas with sufficiently different HPBW might also affect to our values. Regarding the models accuracy, the highest  $\sigma$  is obtained for the FI model,  $\sigma_{FI} = 9.65$  dB, as a consequence of not taking into account the distance. When this factor is introduced in the model, the  $\sigma$  reduces around 3.5 dB. On the other hand, models based on the setup geometry such as 3GPP-A and 3GPP-B provide worse results, with MSEs about 8.9 dB, i.e. 2.7 dB higher than the standard deviation of the frequency and distance dependent models (CI, ABG, and CIF).

#### IV. CONCLUSIONS

The inclusion of human blockage effects in next-generation channel models is essential to accurately predict the wireless propagation behavior, especially at the sub-THz bands. To the best of the authors' knowledge, this work has conducted for the first time a measurement campaign to study the effects of human blockage over an extremely wide band from 75 GHz to 215 GHz; including both mmWave and sub-THz frequencies. It has been seen that the extra attenuation due to humans in the range of 1 m to 2.5 m is between 42 dB and 56 dB, drastically affecting the received power. A fit with several models (FI, CI, ABG and, CIF) has been carried out to

describe the blockage gain, obtaining in all cases a frequency loss exponent around 3 and a distance gain factor of 12 dB/m. Finally, they have been compared with the standardized models 3GPP-A and 3GPP-B (based on site-specific geometry), which provide errors around 2.7 dB higher. The obtained results are expected to be helpful for the development of D2D, BAN, and PAN communications systems.

#### REFERENCES

- [1] K. Rikkinen, P. Kyosti, M. E. Leinonen, M. Berg and A. Parssinen, "THz Radio Communication: Link Budget Analysis toward 6G," *IEEE Commun. Mag.*, vol. 58, no. 11, pp. 22-27, 2020.
- [2] C. Han, Y. Wang, Y. Li, Y. Chen, N. A. Abbasi, T. Kürner and A. F. Molisch, "Terahertz Wireless Channels: A Holistic Survey on Measurement, Modeling, and Analysis," *IEEE Commun. Surv. Tutor.*, vol. 24, no. 3, pp. 1670-1707, 2022.
- [3] S. Dang, O. Amin, B. Shihada and M. S. Alouini, "What should 6G be?," *Nat. Electron.*, vol. 3, pp. 20-29, 2020.
- [4] J. B. Andersen, T. S. Rappaport and S. Yoshida, "Propagation measurements and models for wireless communications channels," *IEEE Commun. Mag.*, vol. 33, no. 1, pp. 42-49, 1995.
- [5] R. Piesiewicz, C. Jansen, D. Mittleman, T. Kleine-Ostmann, M. Koch and T. Kürner, "Scattering Analysis for the Modeling of THz Communication Systems," *IEEE Trans. Antennas Propag.*, vol. 55, no. 11, pp. 3002-3009, 2007.
- [6] F. Sheikh *et al.*, "Scattering and Roughness Analysis of Indoor Materials at Frequencies from 750 GHz to 1.1 THz," *IEEE Trans. Antennas Propag.*, vol. 69, no. 11, pp. 7820-7829, 2021.
- [7] K. Guan, H. Yi, D. He, B. Ai and Z. Zhong, "Towards 6G: Paradigm of realistic terahertz channel modeling," *China Commun.*, vol. 18, no. 5, pp. 1-18, 2021.
- [8] P. Karadimas, B. Allen and P. Smith, "Human Body Shadowing Characterization for 60-GHz Indoor Short-Range Wireless Links," *IEEE Antennas Wirel. Propag. Lett.*, vol. 12, pp. 1650-1653, 2013.
- [9] Y. Dalveren, G. Karatas, M. Derawi and A. Kara, "A Simple Propagation Model to Characterize the Effects of Multiple Human Bodies Blocking Indoor Short-Range Links at 28 GHz," *Electron.*, vol. 10, no. 3, p. 305, 2021.
- [10] U. T. Virk and K. Haneda, "Modeling Human Blockage at 5G Millimeter-Wave Frequencies," *IEEE Trans. Antennas Propag.*, vol. 68, no. 3, pp. 2256-2266, 2020.
- [11] *Propagation by diffraction*, Rec. ITU-R P.526-15, International Telecommunications Union, Geneva, Switzerland, 2019.
- [12] G. R. MacCartney, S. Deng, S. Sun and T. S. Rappaport, "Millimeter-Wave Human Blockage at 73 GHz with a Simple Double Knife-Edge Diffraction Model and Extension for Directional Antennas," in *2016 IEEE 84th Vehicular Technology Conference (VTC-Fall)*, Montreal, QC, Canada, pp. 1-6, 2016.
- [13] P. Pathak, W. Burnside and R. Marhefka, "A uniform GTD analysis of the diffraction of electromagnetic waves by a smooth convex surface," *IEEE Trans. Antennas Propag.*, vol. 28, no. 5, pp. 631-642, 1980.
- [14] S. Takagi, K. Matsui, A. Hirata, K. Takezawa and T. Hayashi, "Reflection and Shadowing Loss due to Human Body in 300-GHz-band Wireless Links," in *2022 IEEE International Workshop on Electromagnetics: Applications and Student Innovation Competition (iWEM)*, Narashino, Japan, pp. 126-127, 2022.
- [15] *5G; Study on channel model for frequencies from 0.5 to 100 GHz*, 3GPP TR 38.901, 3rd Generation Partnership Project, 2022.
- [16] E. M. Murtagh, J. L. Mair, E. Aguiar, C. Tudor-Locke, and M. H. Murphy, "Outdoor walking speeds of apparently healthy adults: A systematic review and meta analysis," *Sports Med.*, vol. 51, no. 1, pp. 125-141, 2020.
- [17] W. C. Y. Lee, "Estimate of local average power of a mobile radio signal," *IEEE Trans. Veh. Technol.*, vol. 34, no. 1, pp. 22-27, 1985.
- [18] T. S. Rappaport, Y. Xing, G. R. MacCartney, A. F. Molisch, E. Mellios and J. Zhang, "Overview of Millimeter Wave Communications for Fifth-Generation (5G) Wireless Networks—With a Focus on Propagation Models," *IEEE Trans. Antennas Propag.*, vol. 65, no. 12, pp. 6213-6230, 2017.